Fast Method to Include Parasitic Coupling in Circuit Simulations

B. L. A. Van Thielen (vthielen@esat.kuleuven.ac.be) and
G. A. E. Vandenbosch (vdbosch@esat.kuleuven.ac.be).
KU-Leuven / TELEMIC

Abstract

S-parameter based circuit simulators are used a lot for the design of microwave circuits. The accuracy of these simulators is limited by the fact that they do not take the electromagnetic coupling between the components and transmission lines that compose a circuit into account. In this article we present a technique that enables us to take this coupling into account without increasing the calculation time too much.

1. Introduction

As modern circuits become smaller and the frequencies that they work at become higher, inevitably, parasitic coupling within the circuits starts to influence the behavior of the circuit more and more. Therefore it is necessary to include the influence of mutual coupling in the circuit simulators that are used to design the circuit.

In this paper the circuit is divided transmission lines and discontinuities (semiconductors, passive components and metal discontinuities that are much smaller than a wavelength).

Three software modules calculate couplings between all combinations of transmission lines and discontinuities. The modules use incoming and outgoing waves at the ports, incident fields and radiating currents. They can be easily combined with a normal circuit simulation engine to include mutual coupling.

In this paper, the results of the developed method are compared with those of a standard method of moments. The theory and the corresponding software that implements this standard method are described in [1] , [2] and [3]

2. Coupling between lines

This section explains how coupling between lines can be calculated much faster by using the eigenmodes (traveling waves) that exist on matched transmission lines. Only first order coupling is calculated: the radiation effect of the induced currents is neglected.

The line – line couplings are calculated for each combination of two lines separately, while discarding all other objects in the circuit. For such a combination of two lines the regular method of moments would need to set up and solve the following matrix equation:

$$\begin{bmatrix} Z_{11} & Z_{12} \\ Z_{21} & Z_{22} \end{bmatrix} \begin{bmatrix} I_{1e} \\ I_{2e} \end{bmatrix} = -\begin{bmatrix} E_1 \\ E_2 \end{bmatrix} \tag{1}$$

The four submatrices represent the self-coupling and the coupling between the two lines. The sub index e indicates that this equation yields the exact solution.

The equation can also be solved iteratively:

$$\begin{aligned} n=1) \quad & I_2^{(1)} = 0 \\ n=2) \quad & I_1^{(2)} = -Z_{11}^{-1} E_{1p1} \\ n=3) \quad & I_2^{(3)} = -Z_{22}^{-1} Z_{21} I_1^{(2)} \\ n=4) \quad & I_1^{(4)} = I_1^{(2)} - Z_{11}^{-1} Z_{12} I_2^{(3)} \\ & \vdots \end{aligned} \tag{2}$$

E_{1p1} is the feed's field. This field is caused by a traveling wave that enters at port one of line one. Line one will be called the source line in the remainder of the text. If line 1 is matched at it's ports then this exciting field will induce a traveling wave on the source line:

$$I_1^{(2)} = \frac{e^{-j\beta x1}}{Z_{c1}} V_1^{+} \tag{3}$$

This knowledge can be used to speed up the second step of (2) by avoiding the inversion of the Z_{11} matrix. Using the specific properties of transmission lines we can also accelerate the third step of (2). When a spatial incident Dirac impulse field is applied to an infinitely long transmission line at position x_2 then the response of the line will always be of the form:

$$\begin{aligned} I_{pulse}(x_2) &= A.\left(e^{j.\beta_2.x_2}.U(-x_2) + e^{-j.\beta_2.x_2}.U(x_2)\right) \\ &\quad + I_{pulse}^{ho}(x_2) \\ &= A.I_{pulse}^{fund.}(x_2) + I_{pulse}^{ho} \end{aligned} \tag{4}$$

U(x) is the Heavyside function: the pulse will generate two traveling waves, both starting at the position at which the pulse is applied and traveling towards infinity. I^{ho}_{pulse} are the higher order modes. These will only propagate over a very short distance, comparable to the line's width, and are therefore ignored. If we look at the Dirac impulse as a one-volt source and replace the two semi-infinite pieces of line with two impedances of Z_c ohms then it is easy to see that the amplitude A in (2) will be equal to $1/(2Z_c)$. We can now find the current from a convolution of the impulse response of the line (4) and the incident field on the line ($E_2 = Z_{21} I_1$). For an observation line with N_2 basisfunctions:

$$I_2(n) = \sum_{i=1}^{N_2} I_{pulse}(n-i)\, E_2(i) \tag{5}$$

This current can now be used in step 4 of (2) to improve the estimate of the source line current. If the coupling between the line is not too high then we can stop after step 3. A general rule of thumb is: if the coupling is equal to -x dB then the second order effect on the source line will be –2x dB and on the observation line –3x dB.

The outgoing waves on the observation line can be immediately calculated: $V_3^- = Z_{c2}\, I_2(1)$ and $V_4^- = Z_{c2}\, I_2(N_2)$ because formulas 3, 4 and 5 where deduced for ideally matched lines. The S-parameters for the pair of lines will be:

$$\begin{aligned} S_{31} = S_{13} &= \frac{V_3^- \sqrt{Z_{c1}}}{V_1^+ \sqrt{Z_{c2}}} \\ S_{41} = S_{14} &= \frac{V_4^- \sqrt{Z_{c1}}}{V_1^+ \sqrt{Z_{c2}}} \end{aligned} \tag{6}$$

The method that was described above is much faster than the regular method of moments. Only the Z_{21} submatrix has to be calculated and no matrix inversions have to be performed at all. If the iteration is stopped after the third step then the convolution (5) only has to be calculated for the first and the last basisfunction of the observation line, which results in a further speed increase. Because the formulas are derived for matched lines no extra deembedding step is needed.

3. Coupling between discontinuities

This second module will calculate the couplings between the discontinuities of the circuit. If these discontinuities are small compared to the wavelength and the distance between them is big compared to their size then their radiation behavior is comparable to that of a dipole. In this section we will discuss how dipoles can be used to calculate the coupling between the circuit's discontinuities in a fast, approximate, way. The better the two above-mentioned assumptions are met, the better the approximation will be. The approximation can always be improved by using more dipoles in the component's model. This new method uses far less unknowns than the method of moments.

Data are added to the S-parameter black box model of the component. This data describes the relation between the incoming (port) waves and the currents on the dipoles

$$\begin{bmatrix} i_1 \\ \vdots \\ i_M \end{bmatrix} = \begin{bmatrix} t_{11} & \cdots & t_{1N} \\ \vdots & \ddots & \vdots \\ t_{M1} & \cdots & t_{MN} \end{bmatrix} \begin{bmatrix} v_1^+ \\ \vdots \\ v_N^+ \end{bmatrix} \tag{7}$$

and the relation between incident fields on the dipoles and outgoing waves:

$$\begin{bmatrix} v_1^- \\ \vdots \\ v_N^- \end{bmatrix} = \begin{bmatrix} r_{11} & \cdots & r_{1M} \\ \vdots & \ddots & \vdots \\ r_{N1} & \cdots & r_{NM} \end{bmatrix} \begin{bmatrix} e_1 \\ \vdots \\ e_M \end{bmatrix} \tag{8}$$

The new, extended description of the discontinuity becomes:

$$\begin{bmatrix} V^- \\ I \end{bmatrix} = \begin{bmatrix} S & R \\ T & X \end{bmatrix} \begin{bmatrix} V^+ \\ E \end{bmatrix} \tag{9}$$

In which S is the S-parameter matrix, and R and T are the matrices defined in (7) and (8). The X submatrix describes the reflections of incident fields on the component. Because of these reflections, indirect paths can be formed between 2 discontinuities through other discontinuities. The additional fields that are caused by these indirect paths are small compared to the direct field. Therefore the X submatrix is neglected and thus set to zero.

The incident field on a discontinuity is calculated using the substrate Green's function:

$$E_i = G_{i,j}\; I_j \tag{10}$$

$G_{i,j}$ is a M_j X M_i matrix that is derived from the Green's function for the substrate. E_i and I_j are vectors describing dipole fields and currents for the i'th and j'th discontinuity.

Using the new description we can now combine all the S-matrices of the discontinuities into one big S-matrix, which includes mutual coupling between them:

$$\begin{bmatrix} V_1^- \\ \vdots \\ \\ \vdots \\ V_D^- \end{bmatrix} = \begin{bmatrix} S_1 & R_1G_{1,2}T_2 & R_1G_{1,3}T_3 & \cdots & R_1G_{1,D}T_D \\ R_2G_{2,1}T_1 & S_2 & R_2G_{2,3}T_3 & \ldots & R_2G_{2,D}T_D \\ \vdots & & \ddots & & \\ R_DG_{D,1}T_1 & \cdots & & R_DG_{D,D-1}T_{D-1} & S_D \end{bmatrix} \begin{bmatrix} V_1^+ \\ \vdots \\ \\ \vdots \\ V_D^+ \end{bmatrix} \tag{11}$$

This matrix will be named S_d. It describes all the discontinuities and their mutual interaction through radiation as a single big S-port. By combining it with the line's S-parameters we can eliminate all waves on internal ports. What remains is an S-parameter description, for the whole circuit, between its external ports.

The optimal dipole positions are found through the use of an optimisation routine. They don’t change much as a function of frequency. If the discontinuity has N ports than excitation of each of these ports will generate a distinct field distribution [4]. The optimisation routine tries to position and feed the dipoles in such a way that, at the centre frequency, their total field resembles these field distributions as much as possible in a number of well chosen testpoints. Only the positions of the dipoles are variables for the optimisation: The optimal dipole excitations for a certain position can be found using a least square method.

The T-matrix (the dipole excitations for each port) is calculated for each frequency after the ideal dipole positions have been calculated for the mid-band frequency. This is done using the least square method again.

The R matrix is calculated by making use of the Method of Moments. (MoM). The discontinuity is subjected to an X-polarised incident field, which is constant over its surface. The MoM. calculates the outgoing waves $V_{ref}(i)$ on the discontinuity ports when subjected to this field. R can now be calculated as CT, where C is a diagonal matrix:

$$C_{ii} = \frac{v_{ref}(i)}{\sum_{n=1}^{Nd} T_{i,n} \cos(\alpha_i)} \qquad (12)$$

The method which has been proposed in this section has the advantage that the matrix that has to be solved is not larger than that of a regular circuit calculation, only less sparse. The method of moments would need to use about 50 to 300 extra unknowns for each discontinuity.

4. Numerical results

The modules of the method are first tested separately and the relation between the approximation error and the proximity of the components is investigated. Then a simple circuit is analysed using both the modules and the S-parameters are compared to those calculated with the Method of Moments.

To find the minimum distance at which the line coupling method still yields accurate results the coupling between a pair of parallel lines is calculated for different distances. Both horizontal lines have a length of 18 mm and a width of .61mm (50 ohm). They start at the same X-position. The substrate is 0.635 mm thick and $\varepsilon_r = 9.9$. The coupling was calculated and compared to the standard method of moments (using 80x5 segments for both lines) for three distances: 3mm, 1.5mm and 1 mm. The continuous line in figure 1 is the result using the standard method of moments, the dot-dash line the new method. Ports 1 and 2 are on the observation line, ports 3 and 4 on the source line. Ports 1 and 3 are on the left, ports 2 and 4 on the right. The results are usable up to 1.5mm. The maximum coupling is then -10 dB (S14).

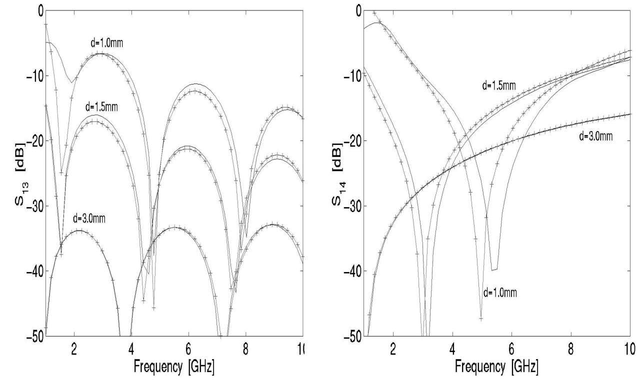

Figure 1. Comparison between M.o.M. and new method (‘+’ line) for coupling between a parallel pair of lines for distances of 1, 1.5 and 3mm. Left: S13, Right: S14

The inter discontinuity coupling module is tested using the T-junction shown in figure 2. A 6 and 3-dipole model is calculated for this discontinuity (with 100 testpoints in a circle with R_t = 4mm) and the fields generated by the models are compared to those of the component as a function of frequency and distance. The calculated model is then used to calculate the S-parameters for the 2 coupled T-junctions.

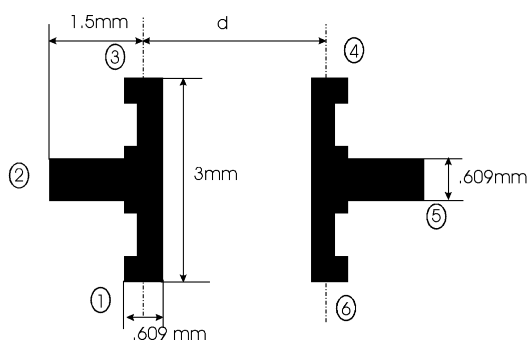

Figure 2. Two T-junctions that will be used to check the inter discontinuity coupling module. Port numbers are indicated

The circuit is placed on a substrate with ε_r = 9.9 and a thickness of .631 mm. For this substrate the lines have a characteristic impedance of 50 ohms. For the M.o.M. both junctions use 88 rooftop basis functions. In all the following figures the T-junction is positioned with its middle leg pointing down. The dipole model can be verified by comparing the field it generates at the testpoints to the original field distribution. This is shown as a function of frequency for a testpoint radius of 4mm in figure 3. The graph shows the ratio of the maximum error (over all testpoints) to the maximum field strength for the 6 (left graph) and 3-dipole (right graph) model.

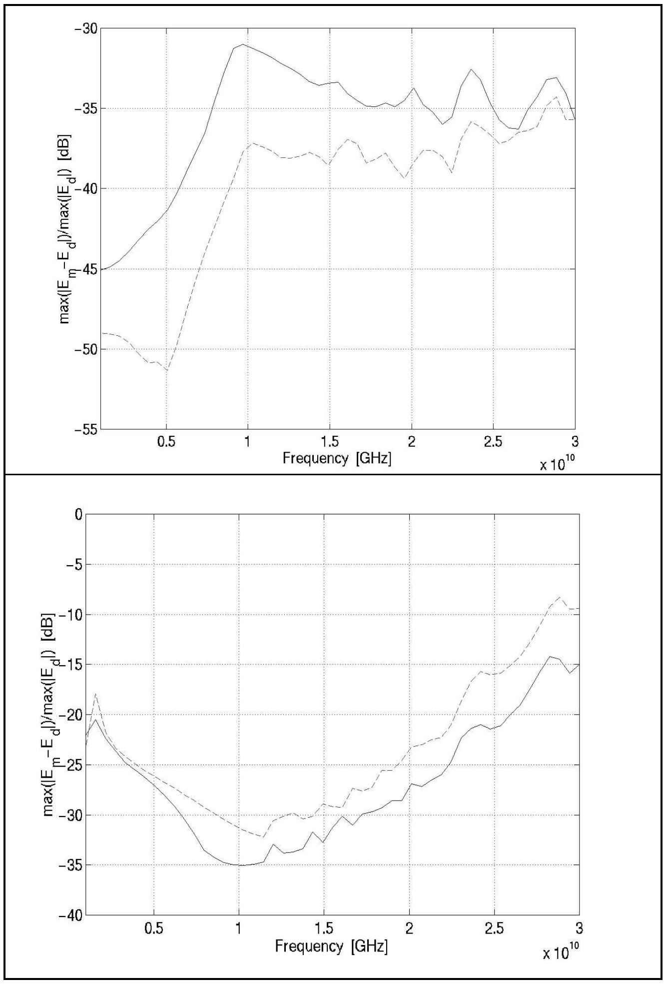

Figure 3. Ratio of maximum error to maximum field strength for the 6 (above) and 3-dipole (below) model over a frequency range of 1 to 30 GHz for d = 3 mm. Continuous line = X-field dashed line = Y-field.

The 6 dipole model is clearly better than the 3 dipole model, especially at high frequencies. The reason for this is that at high frequencies (30GHz) the phase differences across the T-junction become important. The component is becoming larger compared to the wavelength and more dipoles will be needed.

Figure 4 shows the error ratio as a function of the distance between observation point and component at 30 GHz. As expected the error will sharply increase once the distance becomes too small. The error becomes unacceptably high for this 3mm wide T-junction at about 2.3 mm.

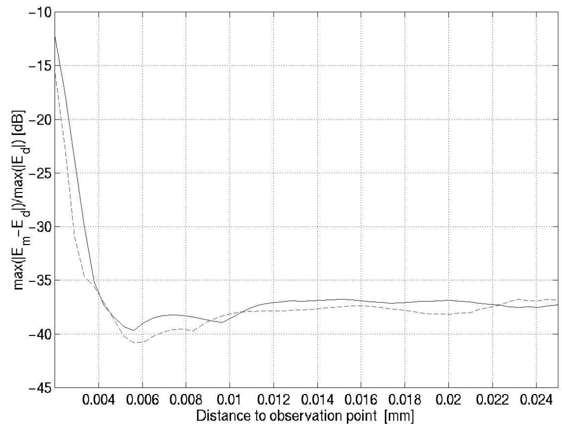

Figure 4. Error ratio for the 6-dipole model at 30GHz as a function of the distance between the model and the observation point. Continuous line = X-field dotted line = Y-field.

The T-junctions in figure 1 will now be fed by 6 lines. Each line is 9.135 mm long and .61mm wide (50 ohm) and is segmented for the M.o.M. with a 3x45 mesh. The S-parameters for this simple circuit are calculated using the new method and compared to the M.o.M. solution.

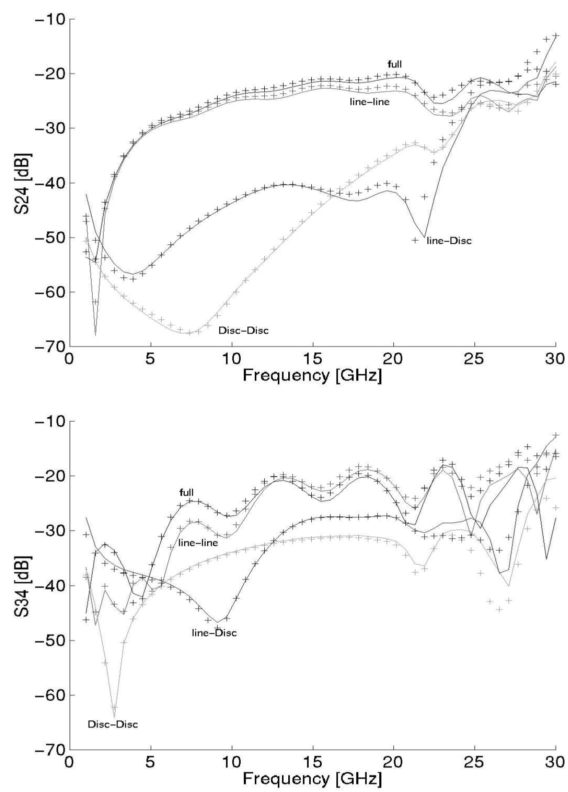

Figure 5. Coupling contributions for T-junctions fed by six lines split up by type. d = 3mm. Continuous line = MoM, '+' line is proposed method.

Figure 5 shows this comparison. The couplings are split up per type: line-line, line-discontinuity, discontinuity-discontinuity, and full coupling. Each graph represents the coupling between two ports. The port numbering is shown in figure 2.

A second example is shown in figure 6.

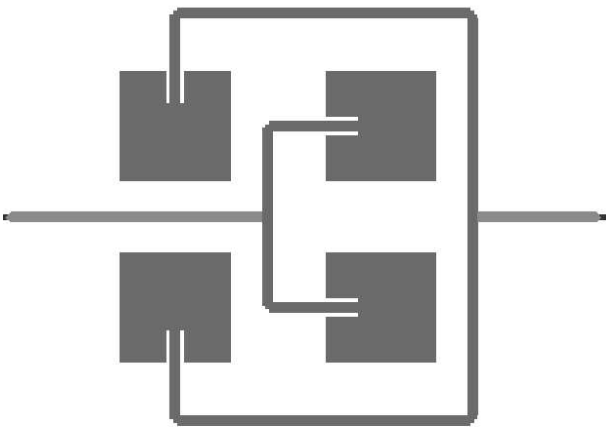

Figure 6. 2x2, dual polarised array of microstrip patch antennas

It proves the validity of the technique for large tightly coupled circuits. The circuit is a 2x2, dual polarisation array of microstrip patch antennas. Each polarisation uses 2 patches. The vertical patches should be fed in couterphase (one element is rotated 180 degrees). To increase coupling between both ports they are fed in phase here. The square patches are 13.4 mm big. The substrate relative permitivity is 2.2 and the substrate height is 1.575mm.

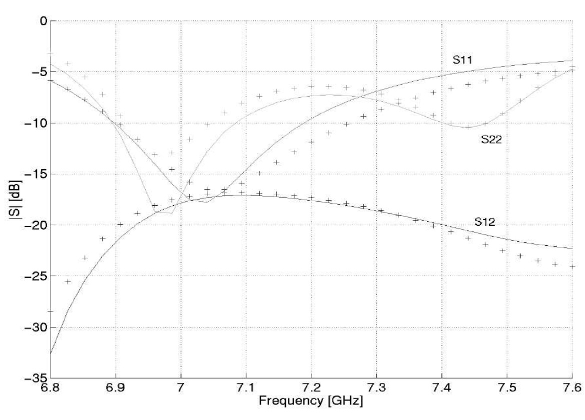

Figure 7. Comparison of S-parameters calculated with MoM (Continuous line) and with proposed method ('+' line) for circuit if figure 6.

The patches are at resonance at 7.2 GHz, at which their impedance is 100 ohm. The characteristic impedance of the transmission lines that are used is 100 ohm. Figure 7 shows a comparison for the S-parameters of this circuit. The left port is port one. The reference planes are put at the T junction and the reference impedance is 100 ohm.

The relatively large differences between both methods are due to the tight coupling between the patch and the first bend (starting from the patch). This coupling is a special case because it consists of a circuit part (coupling between patch and transmission line through the transmission line) and a parasitic part (electromagnetic coupling between patch and bend) . This causes difficulties in the calculation of S11 and S22. This problem is still under investigation.

5. Conclusions

The Main advantage of the method is the speed up. The moment method uses 2.142 seconds to set up its matrix, .345 seconds to solve it and 3.427 seconds to deembed the 6 ports. Only .152 sec are needed for the new method. For large circuits the speed up increases because the inversion time rises proportional to the 3 power of the number of unknowns. The dipole model needs no inversion and will be much faster for large circuits.

Also, the new model needs far less memory than the moment method because only couplings between dipoles of two discontinuities are present in the computers memory.

6. References

1. G. A. E. Vandenbosch and A. R. Van de Capelle, "Mixed-potential integral expression formulation of the electric field in a stratified dielectric medium – Application to the case of a probe current source", IEEE Trans. Antennas Propagat., vol. AP-40, No. 7, pp. 806-817, July 1992.
2. G. A. E. Vandenbosch and A. R. Van de Capelle, "Accurate modeling tool for coaxially fed microstrip patch configurations in stratified dielectric media", Archiv fur Electronik und Ubertragungstechnik, vol. 49, No. 3, pp. 151-159, 1995.
3. B. L. A. Van Thielen and G. A. E. Vandenbosch, "MAGMAS: present status", Proceedings of the COST 245 ESA Workshop on Active Antennas, Noordwijk, The Netherlands, June 1996.
4. K. yang, G. David, J-G. Yook, I. Papapolymerou, L. P. B. Katehi and J. F. Whitaker, "Electrooptic Mapping and Finite-Element Modeling of the Near-Field Pattern of a Microstrip Patch Antenna", IEEE Trans. Microwave Theory Tech., Vol. MTT-48, pp. 288-295, Feb 2000.